Декабрь, № 8. Т. 1 **Физико-технические науки** **2012**

УДК 537.632:621.315.59

ALEXANDER M. GRISHIN
Ph. D., Department of Condensed Matter Physics, Royal Institute of Technology (Stockholm-Kista, Sweden)
grishin@kth.se

TOWARD MAGNETO-OPTICAL LASING MEDIA

Luminescent properties of several Er-doped garnet films as building blocks were compared in all-garnet heteroepitaxial magneto-optical photonic crystals: $La_3Ga_5O_{12}$, Gd_3Ga_5O12, $Y_3Fe_5O_{12}$, $Bi_3Fe_5O_{12}$, and $Bi_{2.97}Er_{0.03}Fe_4Al_{0.5}Ga_{0.5}O_{12}$. Long-lived near-IR luminescence in Er substituted gallium and iron garnet layers used both as Bragg mirrors, and microcavities promise magneto-optical photonic crystals to become an active lasing medium.

Key words: Magneto-optical photonic crystals, garnet materials

INTRODUCTION

Newer photonic integrated circuits (PICs) own variety of functions as lasing, modulation, wavelength multiplexing, etc. integrating all optical components on the same semiconducting platform. Optical isolators are irreplaceable part of PICs. Laser sources are sensitive to feedback – a light backscattered from other elements the laser is coupled and from external elements on the transmission line. Optical isolators prevent unwanted feedbacks providing unidirectional propagation of optical signals. Due to spontaneous magnetization breaking time inversion symmetry $t \rightarrow - t$, ferromagnetic materials demonstrate nonreciprocal Faraday effect: rotation of the plane of polarization of the light in a different direction according to the direction of propagation of the light. Rare earth iron garnets are the principal materials for non-reciprocal passive optical devices in telecommunication applications.

Bismuth substituted rare earth iron garnets combine high Faraday rotation (FR) and transparency in visible and near infrared light. Completely substituted bismuth iron garnet $Bi_3Fe_5O_{12}$ in the form of a single layer epitaxial film keeps the record value of FR $\theta_F = - 8{,}4°/\mu m$ at 633 nm [1], [10]. Further increase of FR was offered by light localization in magneto-optical photonic crystals (MOPCs). Rosenberg's idea [11] to enhance FR by placing MO-material in a resonant cavity has been practically realized in one dimensional (1D) MOPC by Inoue *et al* [5]. Ultimate MO performance was recently achieved in all-garnet MOPCs: 1D heteroepitaxial $Bi_3Fe_5O_{12}/Y_3Fe_5O_{12}$ [6], $Bi_3Fe_5O_{12}/Gd_3Ga_5O_{12}$ [7], $Bi_3Fe_5O_{12}/ Sm_3Ga_5O_{12}$ [4], [8], and $Bi_3Fe_4Al_{0.5}Ga_{0.5}O_{12}/Sm_3Ga_5O_{12}$ [9] crystals. So far, $Bi_3Fe_5O_{12}/Sm_3Ga_5O_{12}$ MOPC with 6 pair quarter-wavelength reflectors in two Bragg mirrors and half-wavelength $Bi_3Fe_5O_{12}$ microcavity in-between demonstrated the highest specific FR $\theta_F = - 20{,}5°/\mu m$ at 750 nm [8]. Even though superior FR, the accompanying high optical absorption hinders practical applications of $Bi_3Fe_5O_{12}$ films. It is still a challenging task to engineer MO crystals which compromise a strong FR with modest optical insertion loss.

Reduction of bismuth concentration and substitution of the Fe^{3+} ion by other trivalent diamagnetic ions strongly suppress light absorption [12], [13]. We employed combined Al, Ga, and Er substitution of, respectively, ferric and bismuth ions to enhance transmissivity and make MOPCs luminescent. In this paper we review our recent results on synthesis and characterization of optical properties of garnet materials and magneto-optical photonic crystals with enhanced transmissivity, remnant Faraday rotation and strong luminescence at room temperature.

EXPERIMENTAL

Erbium-doped ferrimagnetic iron- and diamagnetic gallium-contained garnet films and their multilayers were sintered onto $Gd_3Ga_5O_{12}(111)$ single crystal substrates. $La_3Ga_5O_{12}$ (LGG), $Gd_3Ga_5O_{12}$ (GGG), and $Y_3Fe_5O_{12}$ (YIG) films were prepared by pulsed laser deposition (PLD) whereas $Bi_3Fe_5O_{12}$ (BIG), $Sm_3Ga_5O_{12}$ (SGG), and $Bi_3Fe_4Al_{0.5}Ga_{0.5}O_{12}$ films were grown by rf-magnetron sputtering. The details of pulsed laser deposition and sputtering of garnet films have been published elsewhere, in the works [6] and [4], [8], respectively.

Synthesis and characterization of single layer iron- and gallium contained films should always precede preparation of MOPCs. First, reference epitaxial films were deposited to optimize growth conditions and to determine refractive indices $n(\lambda)$ and deposition rates. Then, MOPCs for the resonance wavelength λ_{res} were grown with corresponding Bragg reflectors having thickness of $\lambda_{res}/4n(\lambda_{res})$ and a microcavity which thickness is a multiple of $\lambda_{res}/2n(\lambda_{res})$.

X-ray diffraction analyses verified morphotropic epitaxial quality of all garnet films [4], [8]. The composition of deposited garnets was controlled by the Rutherford backscattering spectroscopy. Doping with 0,5 at.% of Er (0,1 garnet formula units) corresponds to the following volume concentration of Er^{3+}: $4{,}21\times10^{20}$ cm^{-3} in $Gd_3Ga_5O_{12}$ and $Y_3Fe_5O_{12}$, $3{,}97\times10^{20}$ cm^{-3} in bismuth substituted iron garnets, and $3{,}84\times10^{20}$ cm^{-3} in $La_3Ga_5O_{12}$.

Optical dispersion in garnets within 450 to 1000 nm range was examined using fiber-optic *OceanOptics* PC200 and HR4000 spectrometers. Transmittance vs. λ spectra were normalized to the intensity of the light transmitted through a blank $Gd_3Ga_5O_{12}$ substrate. Photoluminescence (PL) in Er-doped garnets we studied using confocal *LabRam* HR800 Raman microscope with nitrogen cooled InGaAs array (900–1700 nm) at 514,5 nm Ar-laser pumping. Decay of the luminescence at room temperature was measured pumping Er-doped films with square pulse modulated 980 nm laser and detecting 1530 nm PL with the Ge uncooled detector shielded with 2 mm thick Si filter.

To compare PL intensities spectra were normalized to films thickness. Such normalization gives reliable relative estimation for transparent gallium garnets meantime underestimates the effectiveness of PL in iron garnets. Incident Ar-laser light in iron garnets is absorbed completely at film surface at the depth ~ $\lambda/(2\pi\sqrt{|\varepsilon|})$. Dielectric permittivity ε grows rapidly at the absorption edge. Therefore, in Er-doped iron garnets green light generates PL in very shallow film surface layer.

FILMS OPTICAL PROPERTIES

As an example, Figs 1 and 2 present transmission and Faraday rotation spectra in 0,9 μm thick $Bi_{2.9}Er_{0.1}Fe_5O_{12}$ film and in 1,6 μm thick $Bi_{2.97}Er_{0.03}Fe_4Al_{0.5}Ga_{0.5}O_{12}$ film. For all rare earth iron garnets Faraday rotation has a local maximum close to the absorption edge around 520 nm (19 231 cm^{-1}, 2.38 eV). In $Bi_{2.9}Er_{0.1}Fe_5O_{12}$ specific FR has a peak value of θ_F = - 29,9 deg/μm at 535 nm and equals - 1,63 deg/μm at 980 nm. Aluminum-gallium substitution for iron leads to reduction of saturation magnetization and consequent decrease of FR: peak θ_F = - 12,6 deg/μm at 526 nm and - 0,58 deg/μm at 980 nm. Diamagnetic ions substitution for Fe^{3+} significantly increases transmissivity: $Bi_{2.97}Er_{0.03}Fe_4Al_{0.5}Ga_{0.5}O_{12}$ film has the same transmittance as unsubstituted $Bi_{2.9}Er_{0.1}Fe_5O_{12}$ though its thickness is almost twice larger. The absorption coefficient $\alpha = \ln(1/T)/$ $Bi_{2.97}Er_{0.03}Fe_4Al_{0.5}Ga_{0.5}O_{12}$ film thickness is 0,21 dB/μm at 750 nm against 0,62 dB/μm in pure $Bi_3Fe_5O_{12}$ film.

Table 1

Material parameters of $Bi_{2.97}Er_{0.03}Al_{0.5}Ga_{0.5}O_{12}$ garnet (resonance transition wavelength λ_o and frequency ω_o, plasma frequency ω_p and oscillator strength f, half linewidth Γ and parameter of spin-orbit coupling Δ)

Transition	λ_0, nm	$\hbar\omega_0$, eV	$\hbar\omega p\sqrt{f}$, eV	$\hbar\Gamma$, eV	$\hbar\Delta$, eV
First	300	4,14	8,82	$< 10^{-3}$	$< 10^{-3}$
Second	480	2,59	0,84	0,09	0,13
Third	407	3,05	0,84	0,03	0,17

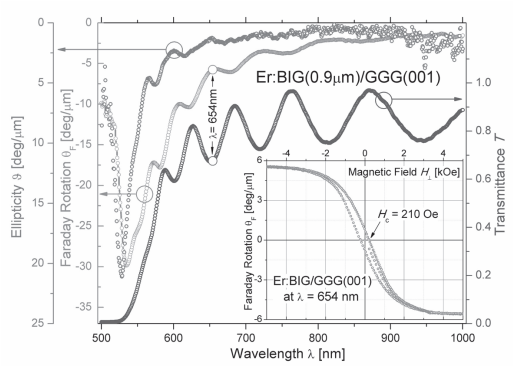

Fig. 1. Transmittance $T(\lambda)$, specific FR $\theta_F(\lambda)$, and ellipticity $\vartheta(\lambda)$ spectra for the 0,9 μm thick $Bi_{2.9}Er_{0.1}Fe_5O_{12}$ film recorded in saturating perpendicular magnetic field H = 3,5 kOe. Inset shows specific FR θ_F[deg/μm] vs. H hysteresis loop traced at the wavelength λ = 654 nm. Two circular symbols ○ depict the magnitudes of the transmittance and FR at this wavelength

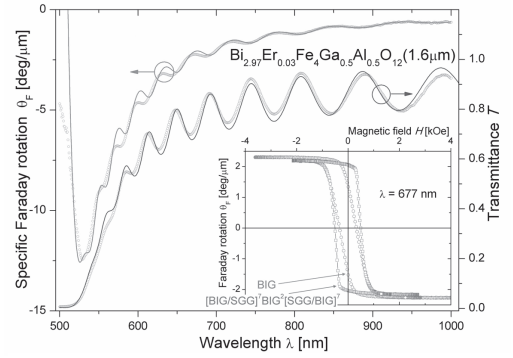

Fig. 2. Transmittance T and specific FR θ_F spectra of the reference 1,6 μm thick $Bi_{2.97}Er_{0.03}Fe_4Ga_{0.5}Al_{0.5}O_{12}$ film. Solid lines show spectra modelled with fitting parameters collected in the Table 1. Inset compares FR θ_F vs. perpendicular magnetic field H hysteresis loops traced at λ = 677 nm in the reference $Bi_{2.97}Er_{0.03}Fe_4Ga_{0.5}Al_{0.5}O_{12}$ film and magneto-optical photonic crystal (MOPC) $[BIG/SGG]^7BIG^2[SGG/BIG]^7$ designed for λ_{res} = 775 nm

The spectra in $Bi_{2.97}Er_{0.03}Fe_4Al_{0.5}Ga_{0.5}O_{12}$ film were fitted (solid lines in Fig. 2) to the theory which accounts three resonance transitions in electric dipole approximation [2]. A complete set of microscopic parameters giving the best fit to the experimental data in $Bi_{2.97}Er_{0.03}Al_{0.5}Ga_{0.5}O_{12}$ garnet is listed in Table 1.

Also, useful interpolation Sellmeier-like formulas for the complex refractive indices can be presented in the wavelength range of our interest as follows for $Sm_3Ga_5O_{12}$ –

$$n^2(\lambda) = 1 + \frac{2.75}{1 - 128\text{nm}/\lambda^2},$$

and for $Bi_{2.97}Er_{0.03}Al_{0.5}Ga_{0.5}O_{12}$ garnet –

$$\left[n(\lambda) - ik(\lambda)\right]^2 = 1 + \frac{4.58}{1-(303\text{nm}/\lambda)^2} + \frac{0.11}{1-(494\text{nm}/\lambda)^2 + i0.08(494\text{nm}/\lambda)}.$$

Besides increased transparency, substitution of ferric ions on tetrahedral positions by diamagnetic Al^{3+} and Ga^{3+} ions induces a perpendicular magnetic anisotropy. Insets in Figs. 1 and 2 show θ_F vs. H hys-

teresis curves recorded under normal incident red laser illumination. Er:$Bi_3Fe_5O_{12}$ film is in-plane magnetized - θ_F vs. *H* loop shows a typical magnetization in the "hard"-axis direction. $Bi_{2.97}Er_{0.03}Al_{0.5}Ga_{0.5}O_{12}$ films demonstrate perpendicular magnetization with characteristic square hysteresis loops and remnant Faraday rotation.

LUMINESCENCE IN GARNET FILMS

As seen in Figs. 1 and 2, the maximum of FR in iron garnets occurs near the absorption edge around 520 nm. Therefore, for new MO-applications we should trade off FR against absorption to achieve superior MO-figure of merit *Q* [deg] = $2\theta_F/\alpha$. As a necessary condition, any method chosen to compensate the absorption of the signal light should not harm the resonant electronic transition (s) responsible for FR. One of the solutions would be to introduce optical gain simultaneously preserving FR.

Er-doped fiber amplifiers, invented in 1987, dominate in commercial WDM signal transmission systems operating in *C*(1530–1565 nm) and *L*(1565–1625 nm) bands. Pumping Er-doped fibers with solid state lasers, the inverted electron population at $^4I_{13/2}$ level can be achieved. As a result, absorption of telecom *C* and *L* optical signal is reduced and optical gain occurs when a pumping overcomes a threshold power. Since Er^{3+} ion easily substitutes any rare earth occupying dodecahedral sites in the garnet structure, both MO-active iron garnet and transparent gallium garnet layers could be grown to host luminescent erbium centers.

Fig. 3 shows photoluminescence spectra in Er-doped films pumped by green Ar-laser. Radiative intra-4*f* Er^{3+} transitions appear to be very different in gallium and iron garnets. The latter films show very strong *C*-band (1530–1565 nm) PL. In Er:$Y_3Fe_5O_{12}$ and Er:$Bi_3Fe_5O_{12}$ at λ_{PL}=1530 nm luminescence, respectively, is 5,2 and 4,1 times stronger than in Er:$La_3Ga_5O_{12}$. On the contrary, at 514.5 nm pumping, intensive luminescence at λ_{PL}=540 and 980 nm caused by radiative transitions from, respectively, $^4S_{3/2}$ and $^4I_{11/2}$ excited Er^{3+} states to the $^4I_{15/2}$ ground state was clearly observed only in Er:$La_3Ga_5O_{12}$ garnet. As seen in the left frame of Fig. 3, PL in Er:$Gd_3Ga_5O_{12}$ in this range is weak and broaden; meanwhile it is completely undetectable for Er:$Bi_3Fe_5O_{12}$ and Er:$Y_3Fe_5O_{12}$. Strong absorption in a broad charge transfer band and weaker one at the resonant $^6A_{1g} \rightarrow {}^4T_{1g}$ transition of octahedrally coordinated Fe^{3+} ion completely extinguishes 540 and 980 nm PL in Er-doped iron garnets.

Two effects are responsible for enhanced *C*-band PL in iron garnets. The first is a strong absorption that pumping green light experiences in iron garnets below 520 nm. The second is the *sensitizing effect*. The $^4I_{11/2}$ energy level of Er^{3+} and the $^4T_{1g}$ level of octahedrally coordinated ferric ion are nearly resonant in energy. Fe^{3+} can be excited either by a pump 514.5 nm Ar-laser in its very broad charge transfer absorption band, or by a solid state 980 nm laser whose light is absorbed at the narrow discrete band around $^4T_{1g}$ level. There are sixteen octahedrally coordinated Fe ions per one Er atom in the erbium substituted iron garnet unit cell. In PL process, the net Fe^{3+} absorption cross section at 980 nm is 16 times higher than that of Er^{3+}. Therefore, pump radiation at 980 nm is efficiently absorbed by Fe^{3+} and then is transferred to Er^{3+}.

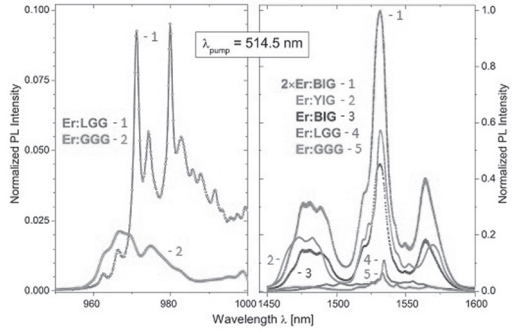

Fig. 3. Comparison of PL spectra in Er-doped garnet films pumped by 514,5 nm Ar-laser. Film compositions $Bi_{2.8}Er_{0.2}Fe_5O_{12}$ (2×Er:BIG), $Bi_{2.9}Er_{0.1}Fe_5O_{12}$ (Er:BIG), $Y_{2.9}Er_{0.1}Fe_5O_{12}$ (Er:YIG), $La_{2.9}Er_{0.1}Ga_5O_{12}$ (Er:LGG), and $Gd_{2.9}Er_{0.1}Ga_5O_{12}$ (Er:GGG) are shown as the shorthands. All the spectra have been normalized to the films thickness. There was no noticeable luminescence observed in 2×Er:BIG, Er:BIG, and Er:YIG iron garnet films at 540 and 980 nm

The analysis of data on *C*-band luminescence decay at room temperature showed, that the excited $^4I_{13/2}$ state lifetime is ranged from 400 μs for Er:$Y_3Fe_5O_{12}$ and 1 ms for Er:$Bi_3Fe_5O_{12}$ to 4 ms for Er:$La_3Ga_5O_{12}$ and almost 6 ms for Er:$Gd_3Ga_5O_{12}$. While pumped by 980 nm laser, the integral *C*-band PL intensity from Er:$La_3Ga_5O_{12}$, Er:$Bi_3Fe_5O_{12}$, and 2×Er:BIG was found to be in the ratio of 0.79:0.49:1 compared to 0.21:0.45:1 at 514 nm pumping (see Fig. 3). It evidences that the 514 nm pumping of Er:$Bi_3Fe_5O_{12}$ films is much more efficient than 980 nm one. We rely this upon incomparable stronger absorption of green light in $Bi_3Fe_5O_{12}$ compared to $La_3Ga_5O_{12}$.

MAGNETO-OPTICAL PHOTONIC CRYSTALS

Erbium ions can be added both to the garnet layers in Bragg reflectors and/or microcavities. This raises a challenging task to engineer Er-substituted all-garnet MOPCs that combine lasing/amplifying and nonreciprocal optical properties with MO remanence. Luminescent MOPCs promise built-in *intelligence*: ability to simultaneously recognize, process and store optical data, make color filtering, and amplify optical signals.

Photoniccrystal(with7$Bi_{2,97}Er_{0.03}Fe_4Al0{,}5Ga_{0.5}O_{12}$ / Sm3Ga5O12 reflec-tors in two Bragg mirrors and half-wavelength $Bi_{2,97}Er_{0,03}Fe_4Al_{0,5}Ga_{0,5}O_{12}$ microcavity in-between designed for 775 nm) spectra have a stop band structure – the band gap with the transmittance central peak at the resonance wavelength λres = 775 nm. Table 2 collects the properties of fabricated MOPC: resonance net Θ_F and specific θ_F

Faraday rotation (the latter is normalized to the total thickness of $Bi_{2.97}Er_{0.03}Fe_4Al_{0.5}Ga_{0.5}O_{12}$ layers notified in the Table 2 with the abbreviation BIG), resonance bandwidth δλ as well as MO-quality factor defined at λ_{res} as Q [deg] = $2|\Theta_F|/\ln(1/T)$. Compared to the reference $Bi_{2.97}Er_{0.03}Fe_4Al_{0.5}Ga_{0.5}O_{12}$ film, MOPC demonstrates enhanced MO properties: specific FR θ_F and quality factor Q were increased, correspondingly, by the factor of 12 and 2. As a band pass filter, 775 nm MOPC possesses narrow bandwidth δλ and a strong light rejection within the stop band characterized by peak-to-valley transmittance ratio as high as 23 dB.

Table 2

Properties of $Bi_{2.97}Er_{0.03}Al_{0.5}Ga_{0.5}O_{12}/Sm_3Ga_5O_{12}$ photonic crystal and reference films ($Bi_{2.97}Er_{0.03}Fe_4Al_{0.5}Ga_{0.5}O_{12}$ is notified with the abbreviation BIG)

Film composition	λ_{res}, nm	MOPC thickness, nm	MO-layers thickness, nm	Resonance bandwidth δλ, nm
[BIG/SGG]^7/ BIG^2/[SGG/BIG]^7	775	2594	1207	3,8
	at 775 nm		1600	
Reference BIG	at 750 nm		700	
	at 640 nm			
Reference $Bi_3Fe_5O_{12}$	at 750 nm			

Film composition	λ_{res}, nm	Resonance FR		Quality factor at λ_{res} $Q = 2\|\Theta_F\|/\ln(1/T)$, deg
		$\|\theta_F\|$, deg/μm	$\|\Theta_F\|$, deg	
[BIG/SGG]^7/ BIG^2/[SGG/BIG]^7	775	14,1	17,0	99,3
	at 775 nm	1,2	1,9	57,0
Reference BIG	at 750 nm	1,6	2,6	68,7
	at 640 nm	3,3	5,3	42,0
Reference $Bi_3Fe_5O_{12}$	at 750 nm	3,6	2,5	50,0

Single layer $Bi_{2.97}Er_{0.03}Fe_4Al_{0.5}Ga_{0.5}O_{12}$ film and $Bi_{2.97}Er_{0.03}Fe_4Al_{0.5}Ga_{0.5}O_{12}/Sm_3Ga_5O_{12}$ MOPC have out-of-plane magnetization. As it is seen in inset to Fig. 2, squareness of magnetization loop increased for MOPC and remnant (latched) Faraday rotation appeared as large as 95 % of the saturated value. Strengthening of perpendicular anisotropy in MOPC compare to a reference $Bi_{2.97}Er_{0.03}Fe_4Al_{0.5}Ga_{0.5}O_{12}$ film, we rely upon the in-plane compressive strain and corresponding out-of-plane rhombohedral distortions of $Bi_{2.97}Er_{0.03}Fe_4Al_{0.5}Ga_{0.5}O_{12}$ unit cell. In a single layer $Bi_{2.97}Er_{0.03}Fe_4Al_{0.5}Ga_{0.5}O_{12}$ film, a strain induced by a large film-to-substrate lattice mismatch releases through a nucleation of copious misfit dislocations leading to cracks in thicker films. In multilayered garnet films, finite thickness of layers hinders a nucleation of misfit dislocations. As a result, mismatch strain is accumulated while a magnetostriction converts it to the uniaxial magnetic anisotropy.

Normalized *C*–band PL spectra in 7-reflectors MOPC and single layer $Bi_{2.97}Er_{0.03}Fe_4Al_{0.5}Ga_{0.5}O_{12}$ film of the same effective thickness were compared. Both samples have sharp emission peaks related to the main $^4I_{13/2} \rightarrow {}^4I_{15/2}$ laser transition. Fine structure of the spectrum reflects Stark splitting of $^4I_{13/2}$ and $^4I_{15/2}$ manifolds of dodecahedral coordinated Er^{3+} ions. Peak PL intensity in MOPC decreased compare to a single layer $Bi_{2.97}Er_{0.03}Fe_4Al_{0.5}Ga_{0.5}O_{12}$ film by a factor of 1.6. This is related to a larger total thickness of the MOPC (2.6 against 1.2 μm).

C–band PL decay curves in 7-reflectors MOPC and reference $Bi_{2.97}Er_{0.03}Fe_4Al_{0.5}Ga_{0.5}O_{12}$ film were compared. Both experimental time dependencies are fitted to the exponential decay with two lifetimes. The main PL component in a single layer $Bi_{2.97}Er_{0.03}Fe_4Al_{0.5}Ga_{0.5}O_{12}$ and MOPC has a magnitude of 96 % and 97 % and is quenched at 700 μs and 600 μs, respectively. Long-life component survives within 1,8 ms in Er:$Bi_{2.97}Er_{0.03}Fe_4Al_{0.5}Ga_{0.5}O_{12}$ film and 2,4 ms in MOPC. Longer lifetime in MOPC we rely upon the Er^{3+} excitations in distorted dodecahedral complexes localized at $Bi_{2.97}Er_{0.03}Fe_4Al_{0.5}Ga_{0.5}O_{12}/Sm_3Ga_5O_{12}$ interfaces.

CONCLUSIONS

Long-lived near-infrared PL of Er^{3+} ions at 1530 nm related to the main $^4I_{13/2} \rightarrow {}^4I_{15/2}$ laser transition occurs in Er-doped rare earths/bismuth iron and gallium garnet epitaxial films. Intensive PL at room temperature suggests that a number of different pumping and lasing schemes can be realized through the proper design of Er-doped $Bi_3Fe_5O_{12}/RE_3Ga_5O_{12}$ magneto-optical photonic crystals. Optical gain combined with high FR can be achieved localizing light either in optically dense Er:$Bi_3Fe_5O_{12}$ cavity or in Er:$Bi_3Fe_5O_{12}$ mirrors in crystals with transparent Er:$RE_3Ga_5O_{12}$ cavities.

Al and Ga substitution of ferric ions in $Bi_3Fe_5O_{12}$ garnet reduces optical absorption by a factor of 3 and induces perpendicular magnetic anisotropy. Photonic crystals earn a record high magneto-optical quality and remnant Faraday rotation. At λ_{res} = 775 nm, specific FR $\theta_F = -14{,}1$ deg/μm and MO-quality factor Q = 99,3 deg exhibit the highest to date MOPC performance. Owning gain [3], luminescent all-garnet heteroepitaxial photonic crystals promise great potential for MO memory, light guiding, filtering and switching, exceptional dispersion, nonreciprocal properties as well as integration with semiconductor platforms.

ACKNOWLEDGMENT

The author wishing to acknowledge financial support from the Swedish Research Council (Vetenskapsrådet) through the Advanced Optics and Photonics (ADOPT) Linné center grant and Ministry of Education and Science of Russian Federation Program «Scientific and Educational Community of Innovation Russia (2009–2013)» through contracts № 14.740.11.0895.

REFERENCES

1. Adachi N., Denysenkov V. P., Khartsev S. I., Grishin A. M., Okuda T. Epitaxial $Bi_3Fe_5O_{12}$(001) films grown by pulsed laser deposition and reactive ion beam sputtering techniques // J. Appl. Phys. 2000. Vol. 88. № 5. P. 2734–2739.
2. Dzibrou D. O., Grishin A. M. Fitting transmission and Faraday rotation spectra of $[Bi_3Fe_5O_{12}/Sm_3Ga_5O_{12}]^m$ magneto-optical photonic crystals // J. Appl. Phys. 2009. Vol. 106. Is. 4, 043901.
3. Grishin A. M. Amplifying magneto-optical photonic crystal // Appl. Phys. Lett. 2011. Vol. 97. Is. 4, 061116.
4. Grishin A. M., Khartsev S. I., Kawasaki H. 980 nm $Bi_3Fe_5O_{12}/Sm_3Ga_5O_{12}$ magneto-optical photonic crystal // Appl. Phys. Lett. 2007. Vol. 90. Is. 19, 191113.
5. Inoue M., Arai K., Fujii T., Abe M. Magneto-optical properties of one-dimensional photonic crystals composed of magnetic and dielectric layers // J. Appl. Phys. 1998. Vol. 83. Is. 11, 6768.
6. Kahl S., Grishin A. M. Enhanced Faraday rotation in all-garnet magneto-optical photonic crystal // Appl. Phys. Lett. 2004. Vol. 84. № 9. P. 1438–1440.
7. Khartsev S. I., Grishin A. M. $[Bi_3Fe_5O_{12}/Gd_3Ga_5O_{12}]^m$ magneto-optical photonic crystals // Appl. Phys. Lett. 2005. Vol. 87. Is. 12, 122504.
8. Khartsev S. I., Grishin A. M. High performance $[Bi_3Fe_5O_{12}/Sm_3Ga_5O_{12}]^m$ magneto-optical photonic crystals // J. Appl. Phys. 2007. Vol. 101. Is. 5, 053906.
9. Khartsev S. I., Grishin A. M. High performance latching-type luminescent magneto-optical photonic crystals // Optics Letters. 2011. Vol. 36. Is. 15. P. 2806–2808.
10. Okuda T., Koshizuka N. et al. Synthesis of new magnetooptical material, bismuth iron garnet // IEEE Translation Journal on Magnetics in Japan. 1988. Vol. 3. Is. 6. P. 483–484.
11. Rosenberg R., Rubinstein C. B., Herriot D. R. Resonant optical Faraday rotator // Appl. Opt. 1964. Vol. 3. P. 1079–1083.
12. Scott G. B., Lacklison D. E. Magnetooptic properties and applications of bismuth substituted iron garnets // IEEE Transactions on magnetics. 1976. Vol. 12. Is. 4. P. 292–311.
13. Scott G. B., Lacklison D. E., Page J. L., Hewett J. Absorption spectra and magnetooptic figure's of merit in the $Bi_xSm_{3-x}Fe_{5-y}Ga_yO_{12}$// Appl. Phys. 1976. Vol. 9. P. 71–77.